AD-A130 173 DEPENDENCE OF ADAPTIVE ARRAY PERFORMANCE ON CONVENTIONAL ARRAY DESIGN(U) OHIO STATE UNIV COLUMBUS ELECTROSCIENCE LAB I J GUPTA ET AL. FEB 83 ESL-711679 1/1

UNCLASSIFIED RADC-TR-83-28 F30602-79-C-0068 F/G 17/4 NL

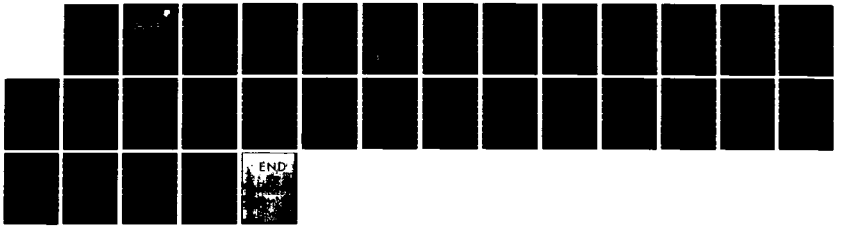

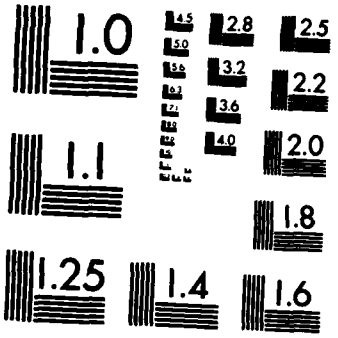

12

RADC-TR-83-28
Interim Report
February 1983

DEPENDENCE OF ADAPTIVE ARRAY PERFORMANCE ON CONVENTIONAL ARRAY DESIGN

The Ohio State University

Inder J. Gupta and A. A. Ksienski

APPROVED FOR PUBLIC RELEASE; DISTRIBUTION UNLIMITED

ROME AIR DEVELOPMENT CENTER
Air Force Systems Command
Griffiss Air Force Base, NY 13441

This report has been reviewed by the RADC Public Affairs Office (PA) and is releasable to the National Technical Information Service (NTIS). At NTIS it will be releasable to the general public, including foreign nations.

RADC-TR-83-28 has been reviewed and is approved for publication.

APPROVED: Stuart H. Talbot

STUART H. TALBOT
Project Engineer

APPROVED: B. Beek

BRUNO BEEK, Technical Director
Communications Division

FOR THE COMMANDER: John P. Huss

JOHN P. HUSS
Acting Chief, Plans Office

If your address has changed or if you wish to be removed from the RADC mailing list, or if the addressee is no longer employed by your organization, please notify RADC (DCCR) Griffiss AFB NY 13441. This will assist us in maintaining a current mailing list.

Do not return copies of this report unless contractual obligations or notices on a specific document requires that it be returned.

UNCLASSIFIED

SECURITY CLASSIFICATION OF THIS PAGE (When Data Entered)

REPORT DOCUMENTATION PAGE		READ INSTRUCTIONS BEFORE COMPLETING FORM
1. REPORT NUMBER RADC-TR-83-28	2. GOVT ACCESSION NO. AD-A130173	3. RECIPIENT'S CATALOG NUMBER
4. TITLE (and Subtitle) DEPENDENCE OF ADAPTIVE ARRAY PERFORMANCE ON CONVENTIONAL ARRAY DESIGN		5. TYPE OF REPORT & PERIOD COVERED Interim Report Aug 80 - Aug 81
		6. PERFORMING ORG. REPORT NUMBER ESL 711679
7. AUTHOR(s) Inder J. Gupta A.A. Ksienski		8. CONTRACT OR GRANT NUMBER(s) F30602-79-C-0068
9. PERFORMING ORGANIZATION NAME AND ADDRESS The Ohio State University Electroscience Laboratory Columbus OH 43212		10. PROGRAM ELEMENT, PROJECT, TASK AREA & WORK UNIT NUMBERS 62702F 45196308
11. CONTROLLING OFFICE NAME AND ADDRESS Rome Air Development Center (DCCR) Griffiss AFB NY 13441		12. REPORT DATE February 1983 13. NUMBER OF PAGES 32
14. MONITORING AGENCY NAME & ADDRESS(if different from Controlling Office) Same		15. SECURITY CLASS. (of this report) UNCLASSIFIED 15a. DECLASSIFICATION/DOWNGRADING SCHEDULE N/A

16. DISTRIBUTION STATEMENT (of this Report)

Approved for public release; distribution unlimited

17. DISTRIBUTION STATEMENT (of the abstract entered in Block 20, if different from Report)

Same

18. SUPPLEMENTARY NOTES

RADC Project Engineer: Stuart H. Talbot (DCCR)

19. KEY WORDS (Continue on reverse side if necessary and identify by block number)

Conventional Array Antenna
Adaptive Array
Sidelobes
Array Performance

20. ABSTRACT (Continue on reverse side if necessary and identify by block number)

A direct relationship between conventional array design and the array performance in an adaptive mode is given. It is shown that the basic goals of conventional array design such as low sidelobes and narrow beamwidth have a direct effect on the adaptive array performance and should not be ignored. An expression is obtained showing that the output signal-to-interference-plus-noise ratio (SINR) of an adaptive array is related to the conventional pattern of the array. The above relations are illustrated for both linear

DD FORM 1 JAN 73 1473 EDITION OF 1 NOV 65 IS OBSOLETE

UNCLASSIFIED

SECURITY CLASSIFICATION OF THIS PAGE (When Data Entered)

and nonlinear arrays.

TABLE OF CONTENTS

LIST OF TABLES

LIST OF FIGURES

I. INTRODUCTION

The adaptive array provides significant advantages over the conventional array in both communication and radar systems. It is often, however, assumed that because of its flexibility in using the available array elements the adaptive array can overcome most, if not all, of the deficiencies in the design of the basic or conventional array that is to be used in adaptive mode. One can, therefore, ignore the conventional goals such as low sidelobes and narrow beamwidth in the array design. Recent work has been drawing attention to the fact that this is not so and that very serious problems, such as grating nulls, will arise with improper element distribution and patterns [1]. This work provides further evidence on the dependence of the adaptive array performance on the soundness of the design of the basic or conventional array that is to be used in an adaptiv mode. In particular, expressions are derived showing that the output signal-to-interference-plus-noise ratio (SINR) of an adaptive array is related to the conventional array characteristics as represented by the adaptive array pattern responding to a single desired signal in the absence of any interfering signal.

In Section II we derive the expression for the output SINR of an adaptive array in the presence of a desired signal and multiple interference signals. The expression is given in terms of the conventional pattern of the array. In Section III we consider the specific case of one jammer. Using linear and nonlinear arrays, we illustrate the relation between the conventional pattern and the output SINR. Section IV contains our conclusions.

II. BASIC RELATION BETWEEN SINR AND THE ARRAY PATTERN

We will derive the above relation utilizing the results derived by Baird and Zahm [2]. According to [2] the steady state weight vector W and the output SINR of an N element LMS adaptive array in the presence of narrowband signals are given by:

$$W = KR_n^{-1}U_d^* \tag{1}$$

and

$$SINR = \xi_d U_d^T R_n^{-1} U_d^* \tag{2}$$

where R_n is the covariance matrix of the undesired signals (interference signals and thermal noise), K is a constant, ξ_d is the ratio of the desired signal power to the thermal noise power, and U_d is the desired signal vector of the array defined as:

$$U_d = \begin{pmatrix} f_1(\theta_d, \phi_d, P_d)\, e^{j\rho_{d_1}} \\ f_2(\theta_d, \phi_d, P_d)\, e^{j\rho_{d_2}} \\ \vdots \\ f_N(\theta_d, \phi_d, P_d)\, e^{j\rho_{d_N}} \end{pmatrix} \tag{3}$$

where θ_d, ϕ_d defines the desired signal direction, P_d is the polarization of the desired signal, $f_j(\theta, \phi, P)$ is the pattern response of the j^{th} element to a signal incident from direction (θ,ϕ) with polarization P and ρ_{d_j} is the desired signal phase at the j^{th} element, measured with respect to the coordinate origin.

Assuming that the thermal noise voltages from the array elements are gaussian with zero means and uncorrelated with each other, and the carrier phase of the narrowband signals are uniformly distributed on $(0, 2\pi)$ and are statistically independent of each other and of the thermal noise voltages, the matrix R_n is given by:

$$R_n = \left[I + \sum_{k=1}^{m} \xi_{ik} U_{ik}^{*} U_{ik}^{T} \right] \tag{4}$$

where I is a N x N identity matrix

m is the total number of interfering signals or jammers

ξ_{ik} is the ratio of the k^{th} jammer power to the thermal noise power.

U_{ik} is the k^{th} jammer vector defined as:

$$U_{ik} = \begin{pmatrix} f_1(\theta_{ik}, \phi_{ik}, P_{ik})\, e^{j\rho_{ik_1}} \\ f_2(\theta_{ik}, \phi_{ik}, P_{ik})\, e^{j\rho_{ik_2}} \\ \vdots \\ f_N(\theta_{ik}, \phi_{ik}, P_{ik})\, e^{j\rho_{ik_N}} \end{pmatrix} \tag{5}$$

where the notation is analogous to that for the desired signal vector.

In the absence of all jammers, the matrix R_n will be an identity matrix and the steady state weight vector (1) will be given by

$$W = KU_d^{*}. \tag{6}$$

We see that the weight vector is proportional to the complex conjugate of the desired signal vector. Let us call the radiation pattern of the array (with U_d^* as the weight vector) the unperturbed pattern of the array. Further, the output SINR using Equation (2) will be:

$$SINR = \xi_d U_d^T U_d^* = \xi_d \, |U_d|^2 \tag{7}$$

and is the maximum possible SINR obtained by the array. The presence of jammers will change the matrix R_n and, thus, the output SINR. We will now derive a relation between the unperturbed pattern of the array and its output SINR in the presence of jammers.

The m jammer vectors U_{ik}, k=1,2,..,m will, at most, scan an m-dimensional complex space. Using the Gram-Schmit process [3], we can construct an orthonormal basis e_1, e_2 ... e_m from the U_{ik}'s for the m-dimensional space as follows:

$$e_k = \begin{cases} 0 & \text{if } |E_k| = 0 \\ \dfrac{E_k}{|E_k|} & \text{otherwise} \end{cases} \tag{8}$$

where

$$E_k = U_{ik} - \sum_{n=1}^{k-1} (U_{ik}^T e_n^*) \, e_n \quad . \tag{9}$$

Note that

$$e_1 = \frac{U_{i1}}{|U_{i1}|} \quad . \tag{10}$$

From (9)

$$U_{ik} = \sum_{n=1}^{k-1} (U_{ik}^T e_n^*) \, e_n + |E_k| \; e_k \quad . \tag{11}$$

Let

$$\alpha_{kn} = U_{ik}^T e_n^* \tag{12}$$

$$n = 1, 2 \ldots k$$

$$k = 1, 2 \ldots m,$$

then from (11)

$$U_{ik} = \sum_{n=1}^{k} \alpha_{kn} e_n \, . \tag{13}$$

Substituting (13) in (4)

$$R_n = \left[I + \sum_{k=1}^{m} \xi_{ik} \left(\sum_{n=1}^{k} \alpha_{kn} e_n \right)^* \left(\sum_{\ell=1}^{k} \alpha_{k\ell} e_\ell \right)^T \right] . \tag{14}$$

In the presence of one jammer, i.e. $m=1$,

$$R_n = \left[I + \xi_{i1} |\alpha_{11}|^2 e_1^* e_1^T \right] \quad . \tag{15}$$

We need R_n^{-1} to compute the weight vector (1) and the output SINR (2). To compute R_n^{-1}, we will use the following matrix inversion lemma [4],

$$(A - \alpha Z^* Z^T)^{-1} = A^{-1} - \beta A^{-1} Z^* Z^T A^{-1} \tag{16}$$

where A is a nonsingular N x N matrix, Z is a N x 1 column vector, and α, β are scalars related by

$$\alpha^{-1} + \beta^{-1} = Z^T A^{-1} Z^* \, . \tag{17}$$

Using the matrix inversion lemma to invert R_n in Equation (15), we get:

$$R_n^{-1} = \left[I - \frac{e_1^* e_1^T}{(|\alpha_{11}|^2 \xi_{i1})^{-1} + e_1^T e_1^*} \right] \tag{18}$$

Note that $e_1^T e_1^* = 1$. If $|\alpha_{11}|^2 \xi_{i1} >> 1$, i.e., the jammer-to-thermal-noise ratio is very large, then

$$R_n^{-1} \cong \left[I - e_1^* e_1^T \right] \quad . \tag{19}$$

Similarly, by the repetitive use of the matrix inversion lemma (16) we can find R_n^{-1} in the presence of multiple jammers. Assuming all the jammers are very strong, we obtain, using Equation (14),

$$R_n^{-1} = \left[I - \sum_{k=1}^{m} e_k^* e_k^T \right] \tag{20}$$

and from (2)

$$SINR = \xi_d U_d^T \left(I - \sum_{k=1}^{m} e_k^* e_k^T \right) U_d^* \quad . \tag{21}$$

Let

$$g_d = U_d^T U_d^* \tag{22}$$

and

$$g_k' = e_k^T U_d^* \quad , \tag{23}$$

then from (21), (22), and (23)

$$SINR = \xi_d \left(g_d - \sum_{k=1}^{m} |g_k'|^2 \right) \quad . \tag{24}$$

Now U_d^* is the weight vector of the array for the unperturbed pattern.[+] Therefore, g_d in (22) is the value of the unperturbed pattern in the direction of the desired signal and g_k' in (23) is the projection of unit vector e_k along the weight vector for the unperturbed

[+]We will consider voltage patterns.

pattern. We will now consider the array performance in the presence of a jammer to show the explicit relation between the output SINR and the unperturbed pattern of the array.

III. ADAPTIVE ARRAY PERFORMANCE IN THE PRESENCE OF A DESIRED SIGNAL AND A JAMMER

In the presence of a single jammer, (24) becomes

$$SINR = \xi_d(g_d - |g_1'|^2) \tag{25}$$

where

$$g_1' = e_1^T U_d^* = \frac{U_{i1}^T U_d^*}{|U_{i1}|} \quad . \tag{26}$$

Let

$$g_1 = U_{i1}^T U_d^* \quad , \tag{27}$$

then

$$SINR = \xi_d(g_d - \frac{|g_1|^2}{|U_{i1}|^2}) \quad . \tag{28}$$

We can clearly see the degradation of the SINR with the appearance of the interference. Note that g_1 in (28) is the value of the unperturbed pattern in the jammer direction taking into account the jammer polarization. Thus, from the unperturbed pattern of the array we can find the output SINR of the array for any jammer direction. For example, in the case of a linear array of isotropic elements (28) yields

$$SINR = \xi_d (N - \frac{|g_1|^2}{N}) \quad . \tag{29}$$

If the desired signal and the jammer are incident from the same direction,

$$g_1 = U_{i1}^T U_d^* = N \tag{30}$$

and from (29) the output SINR will be zero.* On the other hand, if the jammer is incident from a direction in which the unperturbed pattern has a null, there will not be any degradation in the output SINR (the second term in the right hand side of (29) is zero). It is intuitively obvious that the array should not be affected by a jammer arriving from a direction where the pattern has a null. When the jammer is incident from any other direction, the output SINR will be degradated. The degradation will be maximum when the jammer appears at the peak of a sidelobe of the unperturbed pattern. The larger the sidelobe level, the larger the degradation.

Figure 1 shows the unperturbed pattern of a linear array of five isotropic elements. The elements are equispaced at a half wavelength distance. The desired signal direction (θ_d) is 90^o. Figure 2 shows the output SINR of the array as a function of the jammer direction (θ_i). We see that when $\theta_i = \theta_d = 90^o$, the output SINR is zero. We get the maximum output SINR for $\theta_i = 66.5^o$ and 113.5^o. These directions correspond to nulls of the unperturbed pattern. The SINR has minima at $\theta_i = 53^o$ and 127^o, and these are the peaks of the sidelobes of the unperturbed pattern. Thus, as predicted by Equation (29), the output SINR is directly related to the unperturbed pattern. The output SINR incurs no degradation at the nulls of the unperturbed pattern. Degradation in the output SINR increases as the jammer moves away from the nulls. The output SINR is minimum when the jammer reaches the peak of a side

*The above expression assumes that $\xi_{i1} >> 1$ and, consequently, the output SINR will be approximately zero. Actually, SINR $\cong \xi_d/\xi_{i1}$.

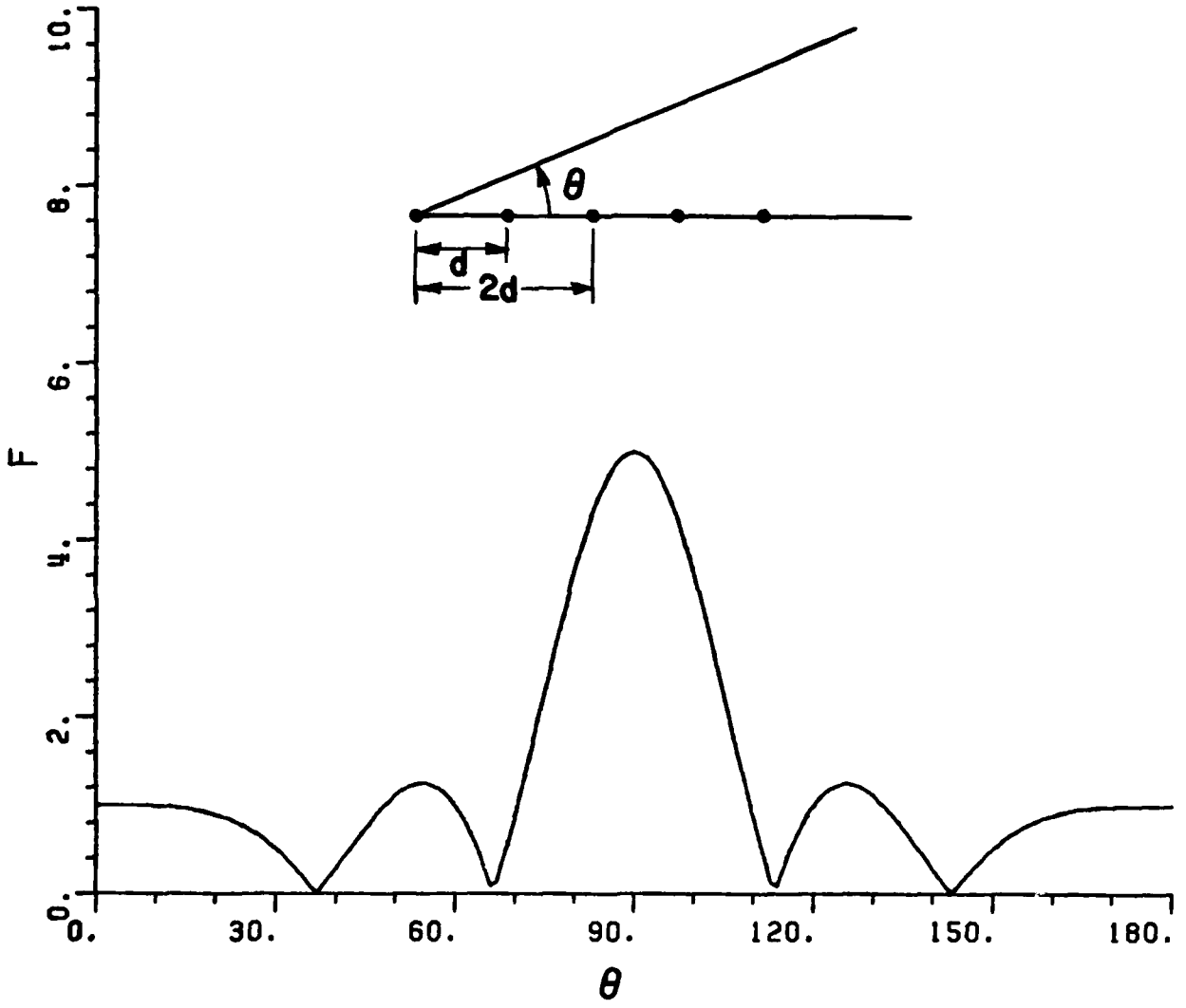

Figure 1. Unperturbed pattern of a linear array of five isotropic elements. $\theta_d = 90^o$, $d = 0.5\lambda$.

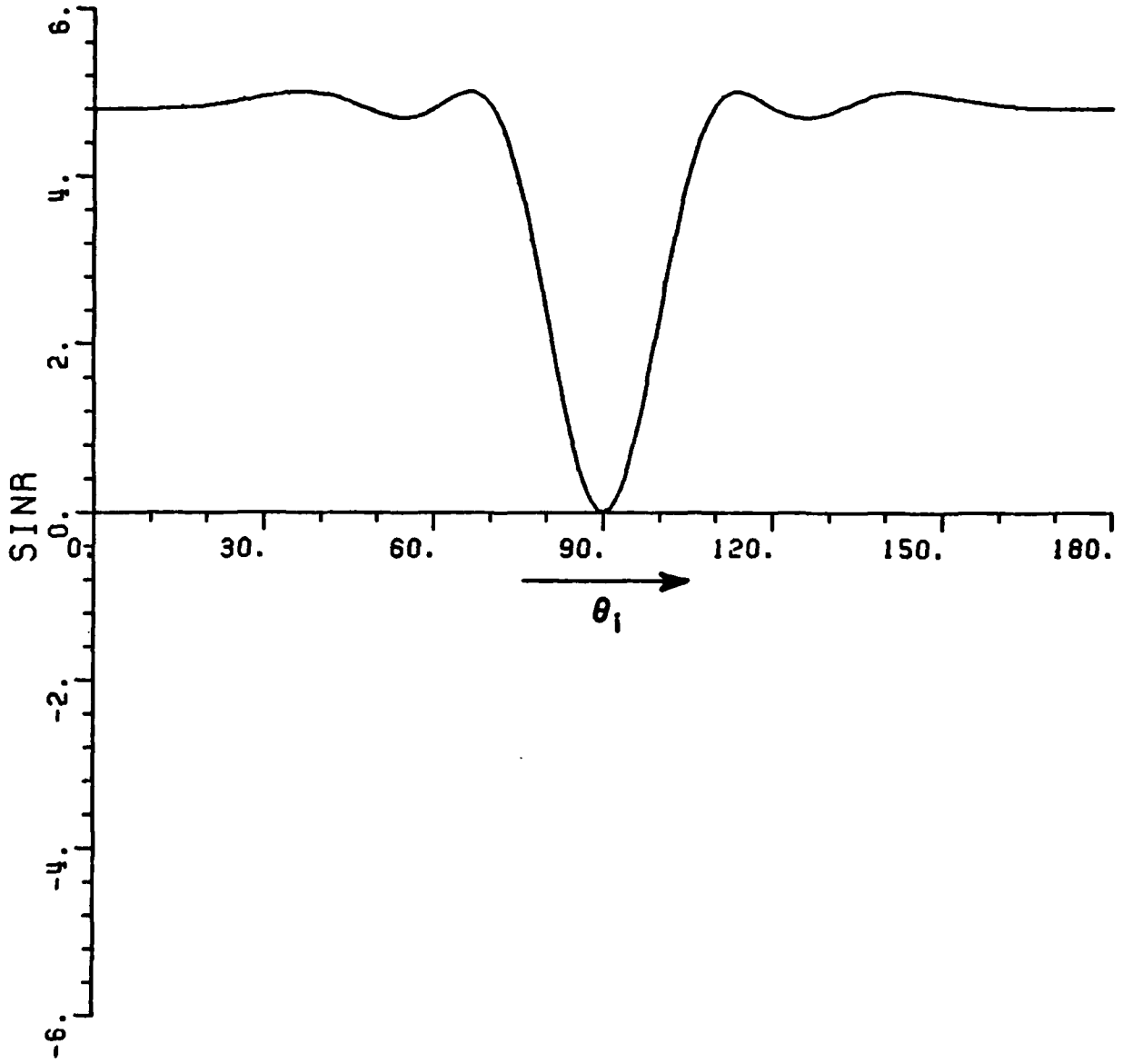

Figure 2. Output SINR of a linear array of five isotropic elements versus θ_1. $\theta_d = 90^o$, $d = 0.5\lambda$, $\xi_d = 1$, $\xi_{il} = 100$.

lobe, with, of course, the global minimum occurring when the jammer reaches the main beam. As the jammer approaches the desired signal direction, the degradation becomes more severe. This points to the fact that the narrower the beam of the unperturbed pattern, the better the resolution of the adaptive array.

Figure 3 shows the unperturbed pattern of the array when the interelement spacing is increased to 0.87λ. We see that the pattern has more sidelobes and the peaks of the sidelobes at 0^0 and 180^0 are quite high. Figure 4 shows the output SINR of the array as a function of the jammer direction. Again, we see that the output SINR is maximum when the jammer direction coincides with one of the nulls in the unperturbed pattern. The output SINR is degraded most when the jammer direction coincides with the beam maximum. The next smaller degradation in the output SINR occurs for $\theta_j = 0^0$ and 180^0 which correspond to the large sidelobe levels in the unperturbed pattern. Thus, sidelobes play an important role in the performance of the adaptive array.

To provide an example of a non-ideal array, we consider a linear array of elements with unequal radiation patterns and interelement spacings. Figure 5 shows the unperturbed pattern of a five-element array. Each element of the array is a short dipole and points in a different direction, i.e., the radiation pattern of the i^{th} element is given by

$$E_i(\theta) = \sin(\theta-\alpha_i) \tag{31}$$

where α_i is the tilt angle of the i^{th} element as shown in Figure 5. The desired signal and the interfering signal are assumed to have the

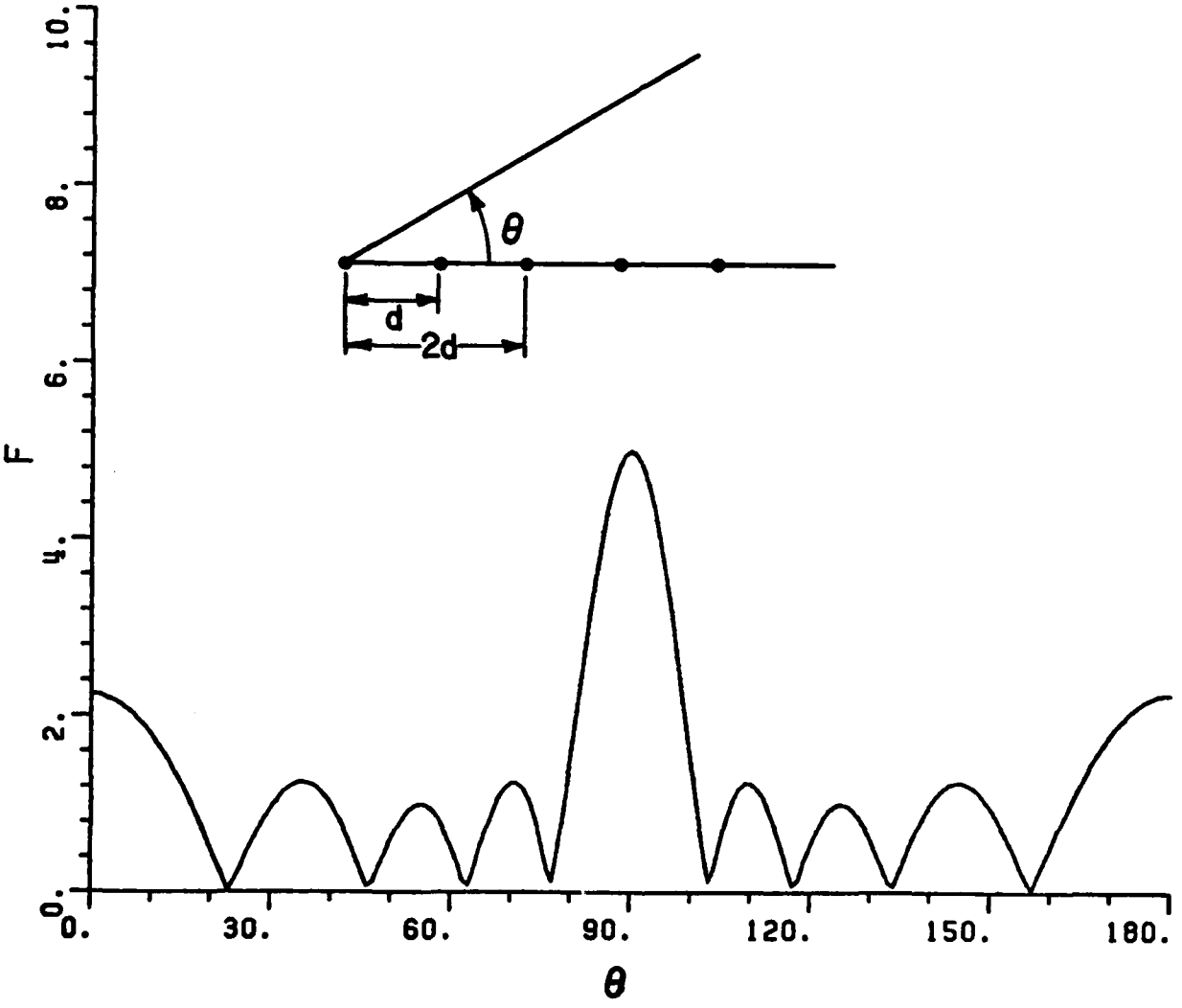

Figure 3. Unperturbed pattern of a linear array of five isotropic elements. $\theta_d = 90^o$, $d = 0.87\lambda$.

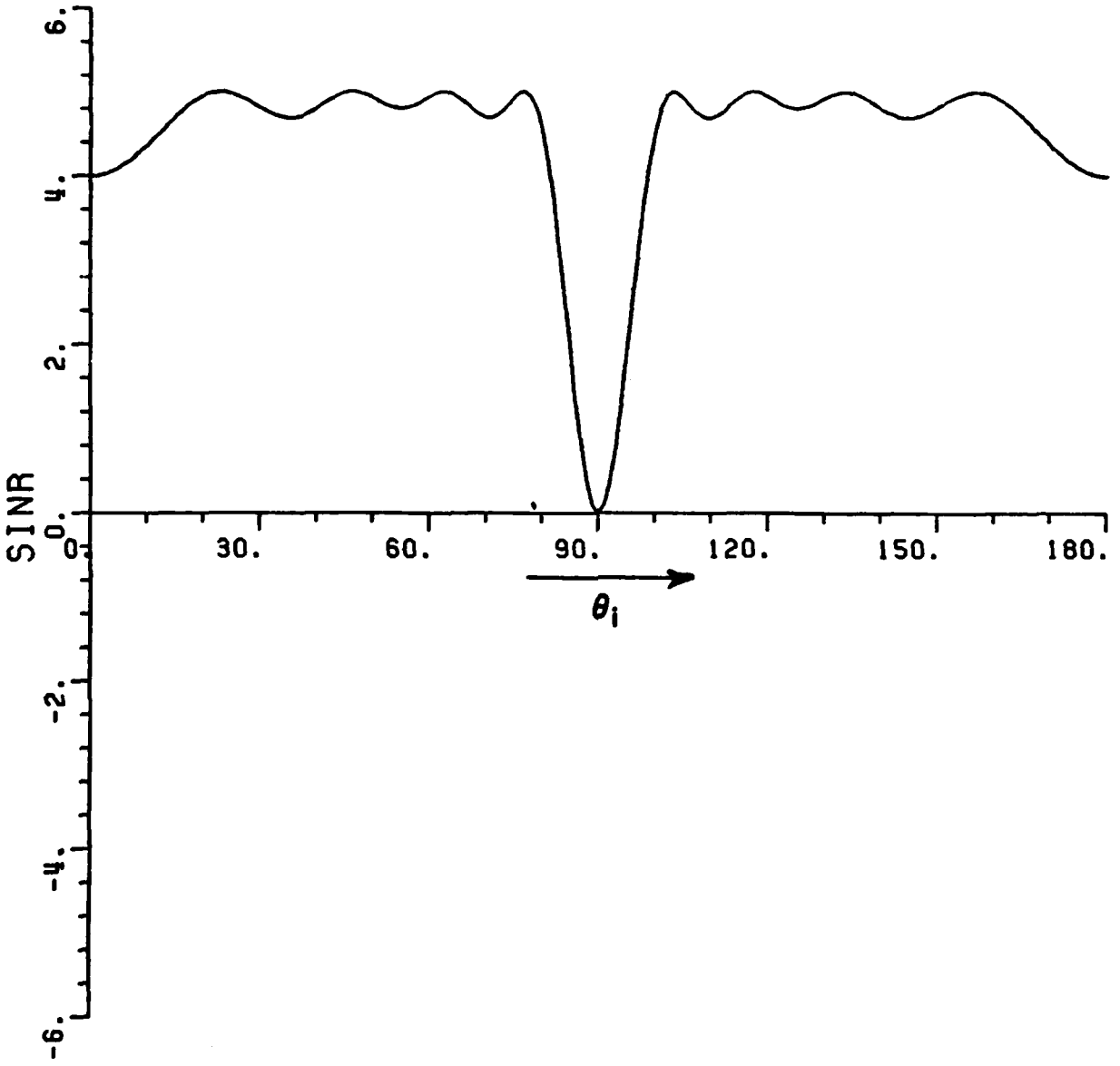

Figure 4. Output SINR of a linear array of five isotropic elements versus θ_i. $\theta_d = 90^0$, $d = 0.87\lambda$, $\xi_d = 1$, $\xi_{i1} = 100$.

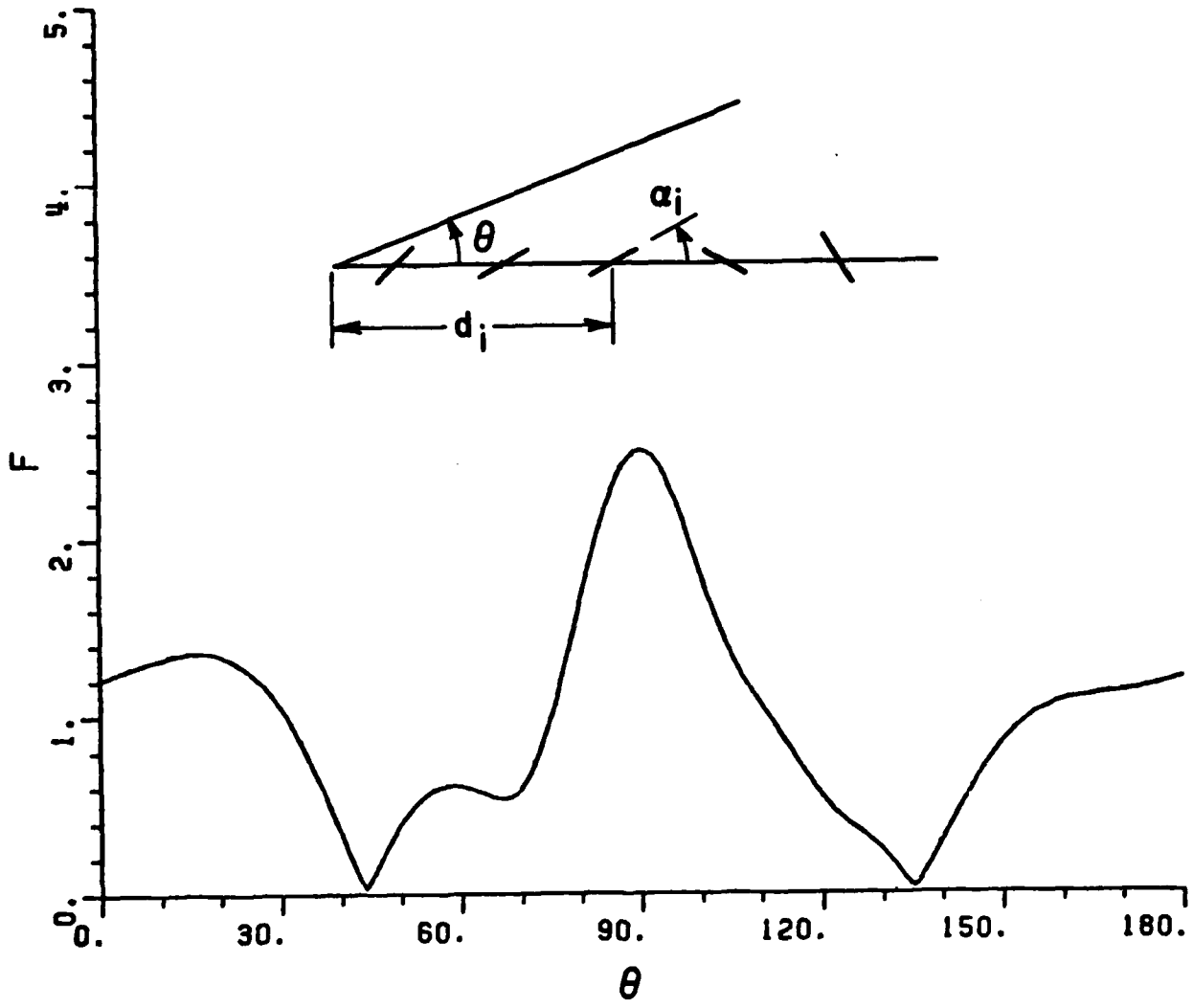

Figure 5. Unperturbed pattern of a linear array of five short dipoles. $d_1 = 0$, $d_2 = 0.4\lambda$, $d_3 = 1.0\lambda$, $d_4 = 1.8\lambda$, $d_5 = 2.8\lambda$, $\alpha_1 = 60°$, $\alpha_2 = 45°$, $\alpha_3 = 0°$, $\alpha_4 = -45°$, $\alpha_5 = -60°$, $\theta_d = 90°$

same polarization. Figure 6 shows the exact SINR of the array (computed using Equation (18), Reference [1]), as a function of jammer direction (θ_j). We see that the output SINR is directly related to the unperturbed pattern (Figure 5) of the array. Table 1 shows the output SINR of the array, calculated using Equation (28) and the unperturbed pattern, for different jammer directions. We see that the SINR calculated using the unperturbed pattern is the same as given in Figure 6. Hence, from the unperturbed pattern of the array, we can find the output SINR of the array.

TABLE 1
OUTPUT SINR OF AN ARRAY OF FIVE DIPOLES

S No.	θ_j	$\|g_1\|$	SINR
1	0^o	1.2	1.925
2	44^o	0	2.5
3	90^o	2.5	0
4	135^o	0	2.5
5	180^o	1.2	1.925

S - Case Number

θ - Angle of Jammer

$|g_1|$ - Gain of Pattern in Unperturbed State in Direction of Jammer

SINR - Signal-to-Inteference-plus-Noise Ratio

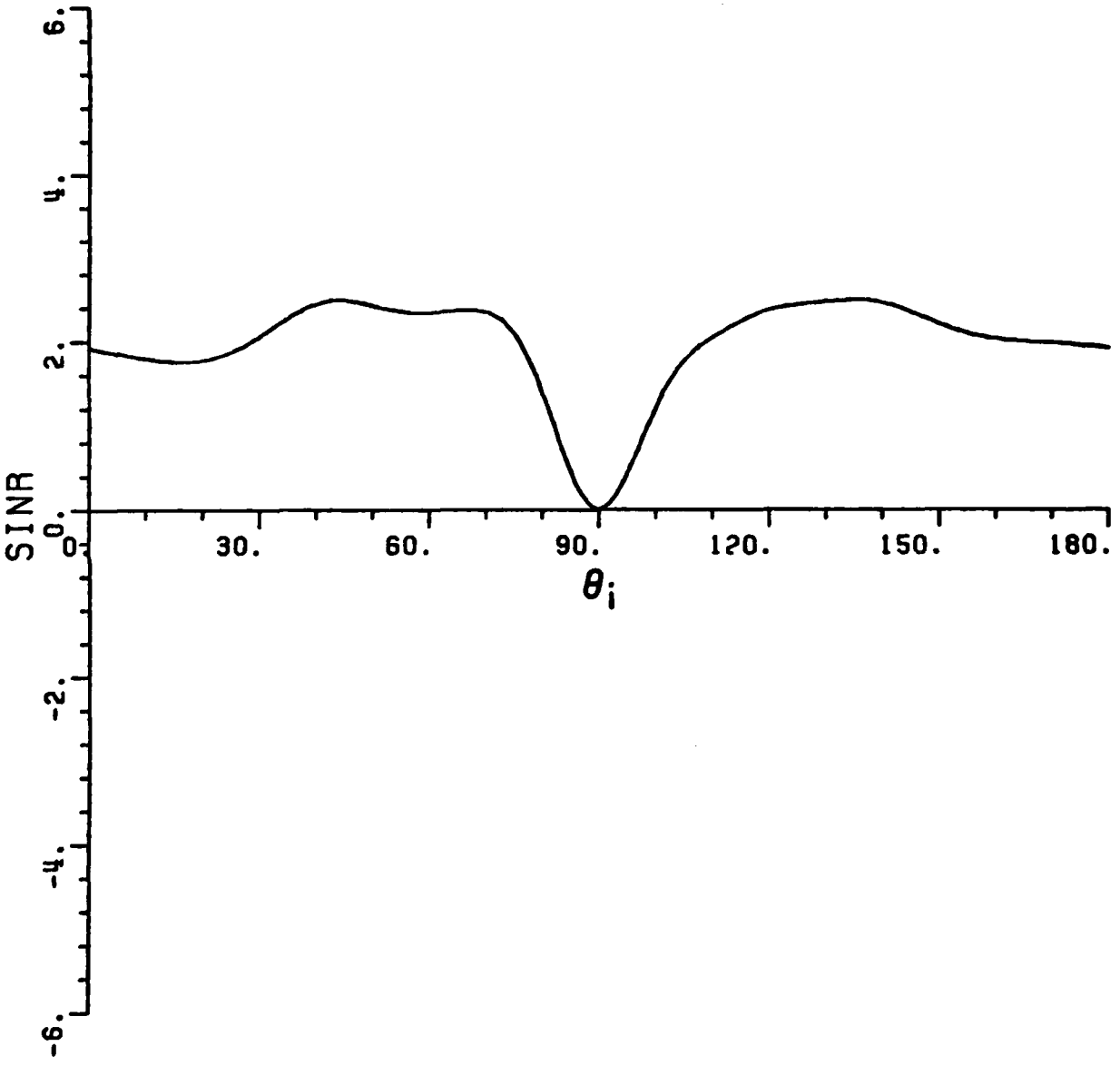

Figure 6. Output SINR of the linear array of Figure 5 versus θ_i. $\theta_d = 90°$, $\xi_d = 1$, $\xi_{11} = 100$

As a last example, let us consider a circular array of isotropic elements as shown in Figure 7. The elements are uniformly distributed around a circle of radius r. Figure 7 shows the unperturbed pattern of a six-element array. The desired signal and the jammer are incident in $\phi = 0$ plane. Figure 8 shows the exact output SINR of the array (computed using Equation (18), Reference [1]), as a function of the jammer direction (θ_j, 0). Again we see that the output SINR is directly related to the unperturbed pattern of the array. Table 2 shows the output SINR of the array, calculated using Equation (28) and the unperturbed pattern (Figure 8), for different jammer direction. We see that the SINR calculated using the unperturbed pattern is the same as given in Figure 8.

TABLE 2
OUTPUT SINR OF A CIRCULAR SIX ELEMENT ARRAY

S No.	θ_j	$\lvert g_1 \rvert$	SINR
1	0^o	2	5.33
2	21^o	3	4.5
3	38^o	0	6
4	90^o	6	0
5	142^o	0	6
6	154^o	3	4.5
7	180^o	2	5.33

S - Case Number

θ - Angle of Jammer

$\lvert g_1 \rvert$ - Gain of Pattern in Unperturbed State in Direction of Jammer

SINR - Signal-to-Interference-plus-Noise Ratio

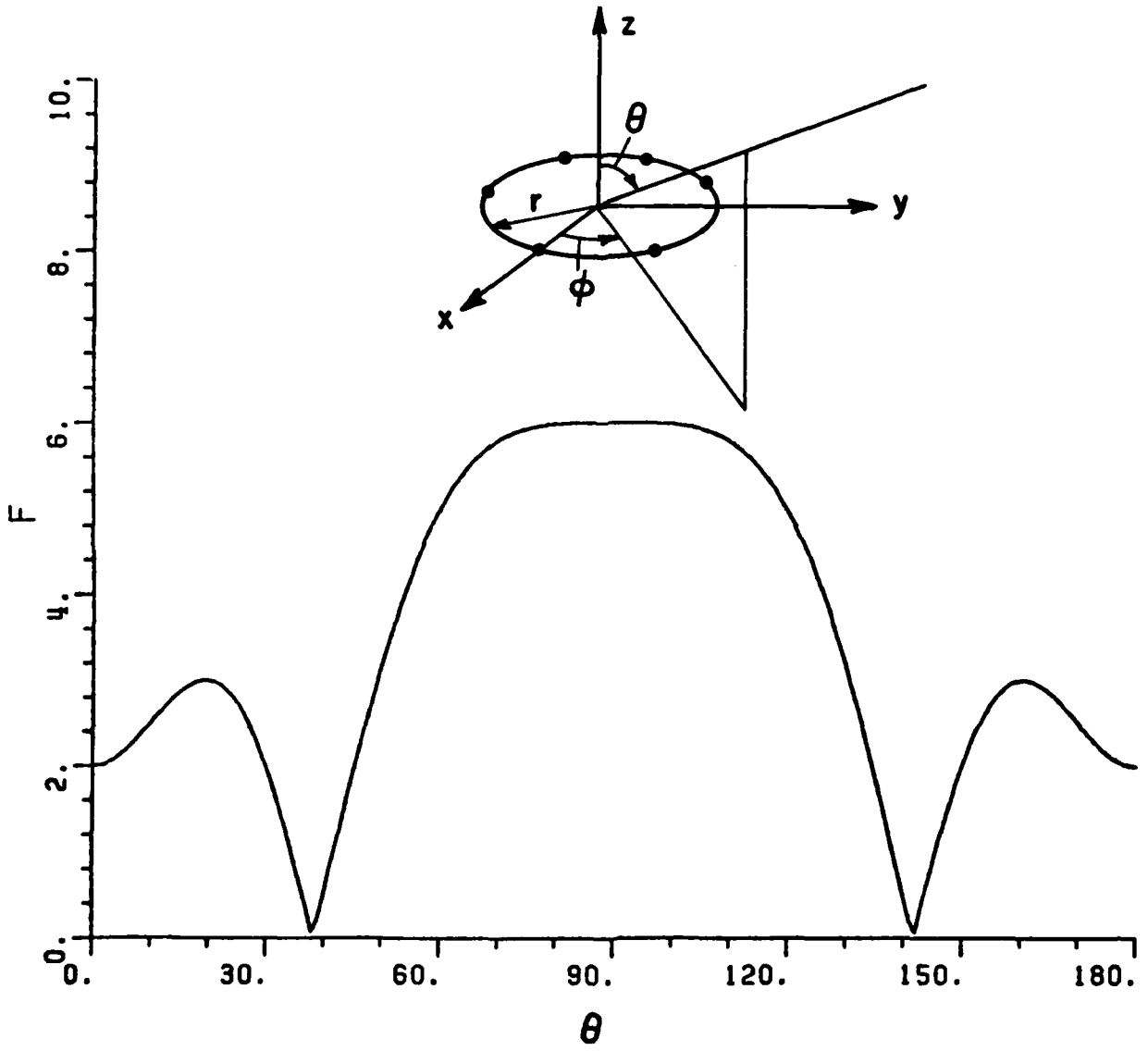

Figure 7. Unperturbed pattern of a six element circular array.
$r = \lambda$, $\theta_d = 90°$, $\phi_d = 0°$, $\phi = 0°$

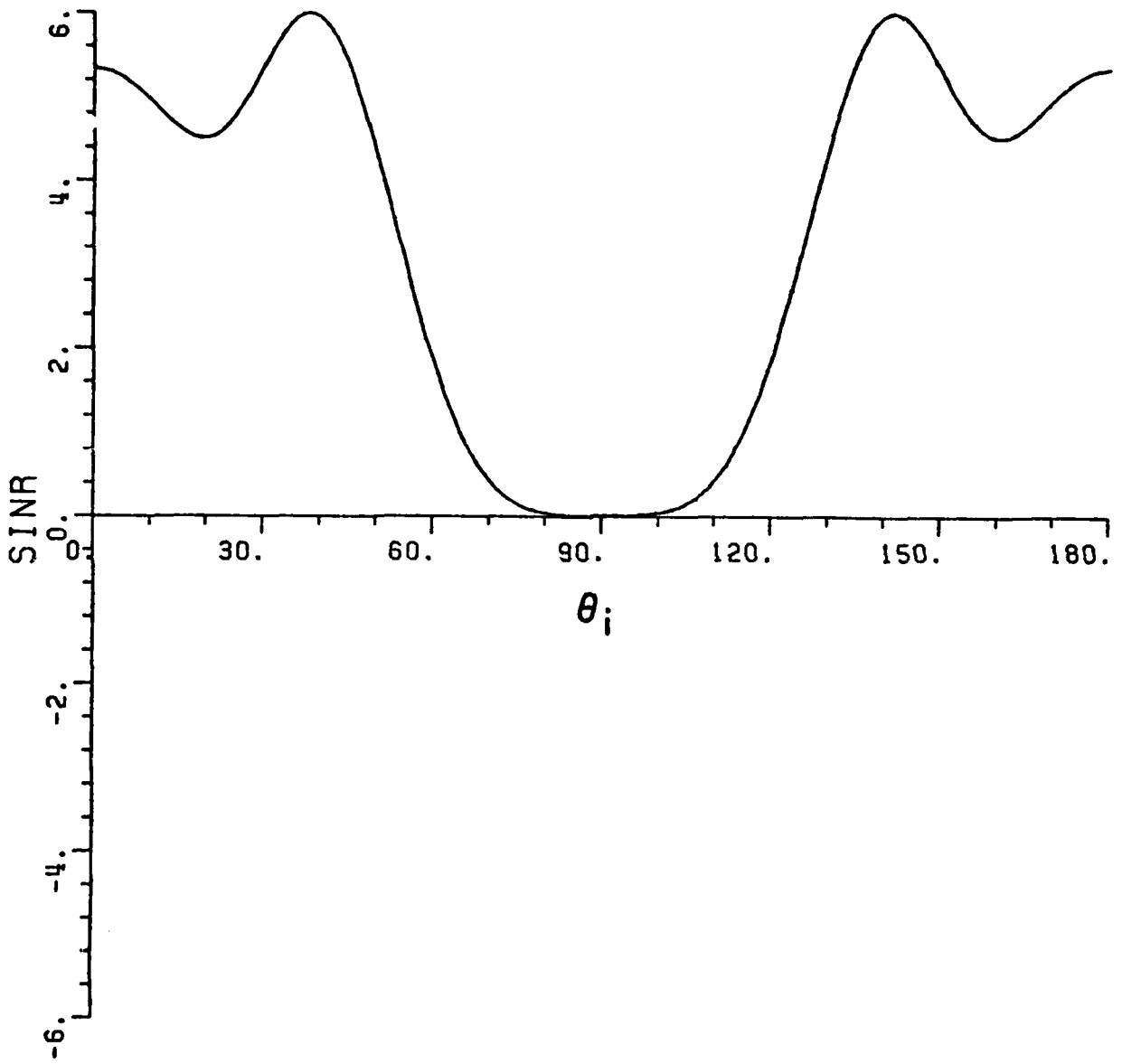

Figure 8. Output SINR of the circular array of Figure 7 versus θ_i. $\theta_d = 90°$, $\phi_d = 0°$, $\phi_i = 0°$, $\xi_d = 1$, $\xi_{jj} = 100$

It should be noted that the amount of degradation is not obtained by the direct subtraction of the sidelobe levels, but is a difference of squares. It can be seen by rewriting Equation (29),

$$\text{SINR} = \xi_d \left(\frac{N^2 - |g_1|^2}{N} \right) \tag{32}$$

For example, if the sidelobe level in the jammer direction is 10% of the main beam (20 dB sidelobe), the reduction in SINR will only amount to 1%. If, however, a large sidelobe is permitted, say 50% of the main beam (6 dB), the reduction in SINR will be 25%. The grating null phenomena [1], in fact, is a particular case in which the sidelobe is permitted to reach the main beam level (0 dB sidelobe). The jammer incident from such a sidelobe direction will cause a null in the output SINR. Since the angular direction of a jammer is a priori unknown, it is apparent that the unperturbed pattern of the array must have low sidelobes to assure good output SINR. In most cases, the desired signal direction is also unknown, i.e. the array must provide coverage over a given sector of space. Under these circumstances, the unperturbed pattern of the array for any θ_d in that sector should have low sidelobes. Thus, the conventional aspects of the array such as gain and sidelobes remain important quantities in array design though an adaptive mode of operation is contemplated. The basic array design should, therefore, strive for both a narrow main beam and low sidelobes for the optimum performance of the adaptive array.

IV. CONCLUSIONS

The objective of the paper was to show the direct relationship between the conventional antenna pattern of an array and its performance

as an adaptive array. Expressions have been provided to obtain the output SINR of the adaptive array in terms of its conventional pattern and the locations of the desired and undesired signals. The most important conclusion to be drawn is that the conventional design goals of low side lobes and narrow main beam have a direct effect on the adaptive array performance and should not be ignored.

REFERENCES

1 A. Ishide and R.T. Compton, Jr., "On Grating Nulls in Adaptive Arrays," IEEE Trans. on Antennas and Propagation, Vol. AP-28, pp. 467-475, July 1980.

2 C.A. Baird, Jr., and C.L. Zahm, "Performance Criterion for Narrowband Array Processing," 1971 IEEE Conference on Decision and Control, Miami Beach, Florida, December 15-17, 1971.

3 J.D. Gilbert, "Elements of Linear Algebra," International Textbook Company, 1970, p. 158.

4 A.S. Householder, "The Theory of Matrices in Numerical Analysis," Dover Publications, Inc., New York, 1964, p. 123.

MISSION
of
Rome Air Development Center

RADC plans and executes research, development, test and selected acquisition programs in support of Command, Control Communications and Intelligence (C^3I) activities. Technical and engineering support within areas of technical competence is provided to ESD Program Offices (POs) and other ESD elements. The principal technical mission areas are communications, electromagnetic guidance and control, surveillance of ground and aerospace objects, intelligence data collection and handling, information system technology, ionospheric propagation, solid state sciences, microwave physics and electronic reliability, maintainability and compatibility.

END

FILMED

8-83

DTIC